Carbohydrate Polymers 87 (2012) 1081–1090

Contents lists available at SciVerse ScienceDirect

Carbohydrate Polymers

journal homepage: www.elsevier.com/locate/carbpol

# Interactions between κ-carrageenan and chitosan in nanolayered coatings—Structural and transport properties

Ana C. Pinheiro[a], Ana I. Bourbon[a], Bartolomeu G. de S. Medeiros[b], Luís H.M. da Silva[c], Maria C.H. da Silva[c], Maria G. Carneiro-da-Cunha[b], Manuel A. Coimbra[d], António A. Vicente[a,*]

[a] IBB – Institute for Biotechnology and Bioengineering, Centre of Biological Engineering, University of Minho, Campus de Gualtar, 4710-057 Braga, Portugal
[b] Departamento de Bioquímica, Laboratório de Imunopatologia Keizo Asami-LIKA, Universidade Federal de Pernambuco, Av. Prof Moraes Rego, s/n, Cidade Universitária - CEP: 50670-420, Recife, PE, Brazil
[c] Green Chemistry Macromolecular and Colloidal Group, Chemistry Department, Federal University of Viçosa, av. P. H. rolfs s/n, Campus UFV, zip code 36570-000, Viçosa, MG, Brazil
[d] QOPNA, Department of Chemistry, University of Aveiro, 3810-193 Aveiro, Portugal

ARTICLE INFO

*Article history:*
Received 3 May 2011
Received in revised form 7 July 2011
Accepted 16 August 2011
Available online 17 September 2011

*Keywords:*
Multilayers
Edible coating
Polyelectrolytes
Electrostatic interactions

ABSTRACT

The interactions between κ-carrageenan and chitosan, two oppositely charged polysaccharides, have been investigated through microcalorimetric and quartz crystal microbalance measurements. Microcalorimetric measurements show that κ-carrageenan/chitosan interaction is an exothermic process and that the alternate deposition of κ-carrageenan and chitosan results in the formation of a nanolayered coating mainly due to the electrostatic interactions existing between the two polyelectrolytes (though other types of interactions may also be involved). Quartz crystal microbalance measurements confirmed that the alternating deposition of κ-carrageenan and chitosan resulted in the formation of a stable multilayer structure. The κ-carrageenan/chitosan nanolayered coating, assembled on a polyethylene terephthalate (PET) support, was characterized in terms of its surface (contact angle measurements) and gas barrier properties (water vapor and $O_2$ permeabilities) and analyzed by scanning electron microscopy (SEM). The water vapor permeability (*WVP*) and the oxygen permeability ($O_2P$) of the κ-carrageenan/chitosan nanolayers were found to be $0.020 \pm 0.002 \times 10^{-11}$ and $0.043 \pm 0.027 \times 10^{-14}$ g m$^{-1}$ s$^{-1}$ Pa$^{-1}$, respectively. These results contribute to a better understanding of the type of interactions that play role during the construction of this type of nanostructures. This knowledge can be used in the establishment of an approach to produce edible, biodegradable multilayered nanostructures with improved mechanical and barrier properties for application in, e.g. food and biomedical industries.



## 1. Introduction

Nanotechnology holds a great potential to generate innovative solutions and to provide food technologists with instruments to meet consumers' demands in very diverse aspects related with foods, such as safety, quality, health-promotion and novelty. Layer-by-Layer (LbL) deposition technique is one of the most powerful methods to create nanolayered coatings with tailored properties (Decher & Schlenoff, 2003). Typically, this technique is based on the alternating deposition of oppositely charged polyelectrolytes and can be applied to produce multilayers of nanometer thickness (1–100 nm per layer) (Weiss, Takhistov, & McClements, 2006). The versatility of the LbL has allowed a deposition of a broad range of materials (e.g. polymers, lipids, proteins, nanoparticles, dye molecules) on various templates (e.g. planar and colloidal) on basis of not only electrostatic interactions but also hydrogen bonding, hydrophobic interactions, covalent bonding and complementary base pairing (Wang, Angelatos, & Caruso, 2007). The functionality of the final films/coatings, such as their permeability to gases, mechanical properties, swelling and wetting characteristics and their environmental sensitivity to pH and temperature, will be determined by the type of adsorbing substances used to create each layer, the total number of layers, the sequence of the different layers and by the conditions (e.g. pH and ionic strength) used to prepare each layer (Weiss, Takhistov, & McClements, 2006). Moreover, the nanolayered coatings can be specially engineered to incorporate bioactive compounds and act as controlled release systems and can be used to coat food products such as fruits and vegetables.

There has been an increasing interest in nanolayered systems due to their potential applications in a wide range of areas including pharmaceutical, biomedical and food packaging. Several

* Corresponding author. Tel.: +351 253 604419; fax: +351 253 678986.
*E-mail address:* avicente@deb.uminho.pt (A.A. Vicente).

0144-8617/$ – see front matter © 2011 Elsevier Ltd. All rights reserved.
doi:10.1016/j.carbpol.2011.08.040

works concerning the production of nanolayered coatings with synthetic polymers (Yoo, Shiratori, & Rubner, 1998) or for biomedical applications (Fu, Ji, Yuan, & Shen, 2005; Martins, Mano, & Alves, 2010) have been done, while few works have used biodegradable polymers from renewable sources and have been directed for the food industry. Examples include the construction of nanolayered coatings composed of poly(L-glutamic acid) and lysozyme (Rudra, Dave, & Haynie, 2006) and of κ-carrageenan and lysozyme (Medeiros, Pinheiro, Teixeira, Vicente, & Carneiro-da-Cunha, 2011), as strategies for food preservation. Therefore, there is a need to create and characterize (e.g. in terms of gas permeabilities) other multilayer systems that combine both biofunctionality and biocompatibility. Biopolymers such as chitosan and κ-carrageenan are competitive candidates for the formation of nanolayered coatings, due to their opposite electrostatic properties, together with their bioactive and non-toxic properties. Chitosan is a natural polysaccharide obtained by deacetylation of chitin, which is the major constituent of the exoskeleton of crustaceous animals, and has been extensively used to produce biodegradable films (Begin & Van Calsteren, 1999; Pranoto, Rakshit, & Salokhe, 2005; Shi et al., 2009). Chitosan is an excellent film component due to its good oxygen barrier properties and due to its intrinsic antimicrobial activity (Begin & Van Calsteren, 1999). κ-carrageenan is a fraction of the sulfated polysaccharides family extracted from certain red seaweeds. It is extensively used in the food industry as gelling, emulsifying, and stabilizing agent and has been reported as having excellent film forming properties (Park, Lee, Jung, & Park, 2001). Polyethylene terephthalate (PET) is a good candidate to be used as a support for the deposition of the polyelectrolytes using the Layer-by-Layer technique due to its excellent physicochemical properties such as good mechanical properties, thermal stability and optical transparency (Fu, Ji, Yuan, & Shen, 2005; Indest et al., 2009).

Understanding the electrostatic interactions of the polyelectrolytes within a nanolayered system can be of utmost importance when considering the development of increasingly specific systems. The driving force for the polyelectrolytes interaction is the enthalpic contribution related to the interaction of oppositely charged groups and the increase in entropy due to the release of their counterions (Vinayahan, Williams, & Phillips, 2010).

The present work aims at evaluating the interactions between κ-carrageenan and chitosan in a nanolayered coating produced through LbL assembly on a PET support and to characterize the nanolayered coating in terms of their permeabilities and surface properties.

## 2. Materials and methods

### 2.1. Preparation of the polyelectrolyte solutions

The κ-carrageenan solution was prepared dissolving 0.2% (w/v) of κ-carrageenan (MW = $3.8 \times 10^5$ Da, 76% purity, GENUGEL carrageenan type WR-78, CPKelco, Denmark) in distilled water under magnetic stirring at approximately 200 rpm during 2 h at room temperature (20 °C). The pH of the solution was adjusted to 7.0 with a solution of 1 M sodium hydroxide (Riedel-de Haën, Germany).

The chitosan solution was prepared dissolving 0.2% (w/v) of chitosan (90% deacetylation, MW = $3.4 \times 10^5$ Da, 99% purity; Aqua Premier Co. Ltd., Thailand) in a 1.0% (v/v) lactic acid (Acros Organics, Belgium) solution under agitation (using a magnetic stirrer) at approximately 200 rpm during 2 h at room temperature. The pH of the solution was adjusted to 3.0 with a solution of 1 M sodium hydroxide (Riedel-de Haën, Germany).

### 2.2. PET aminolysis

PET sheets were obtained from Canson (Annonay Cedex, France) and were cut into rectangular pieces of 0.8 cm × 5.0 cm for the UV–vis, contact angle and SEM analysis and into circular pieces of 5.0 cm of diameter for the gas permeability measurements and were aminolyzed according to previous studies (Fu, Ji, Yuan, & Shen, 2005). Briefly, PET pieces were cleaned through immersion in ethanol (Panreac, Spain)/water (1:1, v/v) solution for 3 h, followed by rinsing with distilled water and drying at 30 °C and at a RH of 42.0 ± 1.5% in an oven for 24 h. Then, the pieces were immersed in 0.06 g $L^{-1}$ 1,6-hexanediamine/propanol (Aldrich-Germany and Sigma–Aldrich-USA, respectively) solution at 37 °C for 4 h, thoroughly washed with distilled water to remove free 1,6-hexanediamine, and finally dried in an oven at 37 °C and at a RH of 42.0 ± 1.5% for 24 h. These aminolyzed PET pieces were treated with 0.1 M hydrochloric acid (Merck, Germany) solution for 3 h at room temperature (20 °C) and then washed with a large amount of distilled water, and dried in an oven at 30 °C and at a RH of 42.0 ± 1.5% for 24 h. The obtained polymer was termed aminolyzed/charged PET (A/C PET).

## 3. Evaluation of the interactions between the polyelectrolytes

### 3.1. Electrostatic properties

The ζ-potential of the polyelectrolyte solutions was calculated by determining the electrophoretic mobility and then applying the Henry equation. The electrophoretic mobility is obtained by performing an electrophoresis experiment on the sample and measuring the velocity of the particles using Laser Doppler Velocimetry (Zetasizer Nano series, Malvern Instruments, UK). The measurements (three readings for each assay) were performed in a folded capillary cell. The assays were performed in triplicate, so the results are given as the average ± standard deviation of the nine values obtained.

### 3.2. Microcalorimetry analyses

For the microcalorimetry analyses, A/C PET pieces were reduced to powder with a mill (Retsch, Germany), at room temperature (20 °C). Calorimetric measurements were carried out using a CSC (Calorimeter Science Corp., USA) microcalorimeter, model 4200 controlled by ItcRun software with a 1.75 mL reaction cell (sample and reference) and sensitivity of 0.02 μW. Determinations of the enthalpy of interactions between chitosan and κ-carrageenan were carried out at 20 °C, in triplicate and the whole calorimetric procedure was chemically and electrically calibrated as recommended (da Silva et al., 2008). During each experiment, aliquots of 10 μL of an aqueous solution of chitosan (0.2% (w/v), pH 3.0) were injected in a sample cell containing (i) 1.75 mL of ultra pure water (dilution enthalpy determination) or (ii) 1.75 mL of a κ-carrageenan aqueous solution (0.2% (w/v), pH 7.0) or (iii) 1.75 mL of a suspension containing 40 mg of A/C PET microspheres with κ-carrageenan adsorbed (adsorbed A/C PET-κ-carrageenan–chitosan apparent interaction enthalpy determination).

For each injection, the experimental heat (enthalpy) change $H_i$ (in kJ) resulting from injection $i$ was obtained by the raw data peak integration. The values of integrated molar enthalpy change for injection $i$, $\Delta H_i$ (in kJ $mol^{-1}$), were obtained by dividing $H_i$ by the number of moles of chitosan added, $n_i$; hence $\Delta H_i = H_i/n_i$. Then, plots of $\Delta H_i$ against the total chitosan concentration added were obtained and are referred as enthalpy curves.

### 3.3. Quartz crystal microbalance analyses

The adsorption behavior of κ-carrageenan and chitosan was evaluated using a quartz crystal microbalance (QCM 200, purchased from Stanford Research Systems, SRS, USA), equipped with AT-cut quartz crystals (5 MHz) with optically flat polished chrome/gold electrodes on contact and liquid sides.

Quartz crystal microbalance (QCM) is one of the few techniques that allow the monitoring of the adsorption process in situ (Indest et al., 2009). It has the ability to sensitively measure mass changes associated with liquid–solid interfacial phenomena, as well as to characterize energy dissipation or viscoelastic behavior of the mass deposited on the electrode surface of the quartz crystal. The principle of the QCM is based on the piezoelectric effect: the mechanical stress applied to the surface of the quartz crystal originates a corresponding electrical potential across the crystal whose magnitude is proportional to the applied stress (Buttry & Ward, 1992). As the mass is deposited onto the crystal surface, the piezoelectric properties of the quartz crystal change its oscillation frequency (Marx, 2003). If the adsorbed material is rigidly attached, evenly distributed and is much thinner than the mass of the quartz crystal, the resulting decrease in the oscillation frequency is proportional to the adsorbed mass and thus can be quantified from the Sauerbrey equation (Sauerbrey, 1959). However, when using polymers, in addition to the measurement of frequency shift, it is necessary to measure the damping of the crystal oscillation, and the previous relation is no longer valid. The Sauerbrey equation can only be used to calculate elastic mass upon the QCM surface after it has been determined experimentally that the bound mass dissipates no energy (Marx, 2003). Other physical parameters can be measured in addition to the resonance frequency, such as motional resistance, which can be used to measure the viscoelastic change of the deposited film. The simultaneous measurements of resonance frequency and motional resistance can differentiate an elastic mass attachment from viscosity-induced effects: for an elastic mass attachment, the motional resistance will be zero and the resonance frequency will be proportional to the mass increase on the surface of the quartz crystal; when viscosity-induced effects are present, the decrease of resonance frequency is accompanied by a proportional increase of motional resistance (Fakhrullin et al., 2007).

Before carrying out the experiments, the crystal was cleaned by successive sonications (40 KHz, 30 min) in ultra pure water, ethanol (Panreac, Spain) and ultra pure water, followed by drying with a gentle flow of nitrogen.

QCM measurements were started with distilled water at pH 7.0 as a baseline. Adsorption measurements were performed by alternate immersion of the crystal in κ-carrageenan (pH 7.0) and chitosan (pH 3.0) solutions, for 15 min. A washing step of 15 min with distilled water (at a pH 7.0 or pH 3.0, depending if the previous adsorption was with κ-carrageenan or chitosan solutions, respectively) was carried out after the deposition of each polyelectrolyte, in order to remove the unbound polyelectrolytes and to prevent the cross-contamination of solutions.

The variations of the resonance frequency ($\Delta F$) and of the motional resistance ($\Delta R$) were simultaneously measured as a function of time and the analyses were performed at 20 °C, in triplicate.

### 3.4. Preparation of nanolayered coating

The nanolayered coating was composed of an A/C PET support layer adsorbed with a polysaccharide multilayer constituted of 5 polysaccharide layers (three κ-carrageenan and two chitosan layers).

In order to prepare the nanolayered coating, A/C PET pieces were firstly dipped into the κ-carrageenan solution for 15 min and subsequently rinsed with distilled water at pH 7.0. The samples were dried under a flow of nitrogen. The procedure was repeated, this time using chitosan as the polyelectrolyte and rinsed with distilled water at pH 3.0. The dipping/washing/drying process was repeated until the deposition of a total of 5 layers (κ-carrageenan/chitosan/κ-carrageenan/chitosan/κ-carrageenan).

As a result of the immersion into polyelectrolyte solutions, both sides of the A/C PET pieces were coated with the same set of layers. Therefore, for the determination of water vapor and oxygen permeabilities, it was necessary to multiply the thickness value of each of the five layers by 2.

The nanolayered coatings were then maintained at 20 °C and 50% relative humidity (RH) before analyses.

### 3.5. Characterization of the nanolayered coating

#### 3.5.1. UV/VIS spectroscopy

In order to follow the multilayer construction, a UV-VIS spectrophotometer (Jasco 560, Germany) was used to measure the absorbance of the prepared nanolayered coatings at a wavelength of 260 nm. This wavelength was chosen according to other authors (Carneiro-da-Cunha et al., 2010; dos Santos et al., 2003; Wasikiewicz, Yoshii, Nagasawa, Wach, & Mitomo, 2005). Three replicates of each measurement were obtained.

#### 3.5.2. Contact angle measurements

The contact angle of the nanolayered coating surface was measured by the sessile drop method, using a face contact angle meter (OCA 20, Dataphysiscs, Germany). A 2 μL droplet of ultra pure water was placed on the horizontal surface of each film with a 500 μL syringe (Hamilton, Switzerland), with a needle of 0.75 mm of diameter, and observed under the contact angle meter. The contact angle measurements were performed at three different surfaces and at each surface, ten replicates of contact angles were obtained at contact times of 0, 15, and 30 s.

#### 3.5.3. Scanning electron microscopy (SEM)

The surface morphology of the nanolayered coating was examined using scanning electron microscopy (Nova NanoSEM 200, Netherlands) with an accelerating voltage from 10 to 15 kV. Before analyses, all samples were mounted on aluminium stubs using carbon adhesive tape and sputter-coated with gold (thickness of about 10 nm). The SEM images allowed the direct measurement of the layers thicknesses (average of three measurements) using the equipment's image analysis software (XT microscope control software).

#### 3.5.4. Water vapor permeability (WVP) measurements

The methodology used was based on the ASTM E96-92 (ASTM E96-92, 1990) method. The films were sealed on the top of a permeation cell containing 55 mL of distilled water (100% RH; 2337 Pa vapor pressure at 20 °C). The cells were then placed in a desiccator at 20 °C and 0% RH (0 Pa water vapor pressure) containing previously dried silica (105 °C overnight) and were weighed during 10 h at intervals of 2 h, assuming steady-state and uniform water pressure conditions (Ziani, Oses, Coma, & Maté, 2008). In order to ensure uniform relative humidity, fan speeds were installed inside the desiccators. Three replicates were obtained for each sample.

The WVP of the A/C PET and of the A/C PET + 5 nanolayers was estimated using regression analysis from [Eq. 1] adapted from literature (Sobral, Menegalli, Hubinger, & Roques, 2001):

$$\frac{wL}{A\ \Delta P} = WVP \times t \quad (1)$$

where $L$ is the average thickness of the films, $A$ is the permeation area (0.005524 $m^2$). $\Delta P$ is the difference of partial vapor pressure of the atmosphere (2337 Pa at 20 °C) and $w$ as the weight loss.

The *WVP* of the polysaccharide nanolayers was determined by the following equation (Cooksey, Marsh, & Doar, 1999):

$$WVP_B = \frac{L_B}{(L_T/WVP_T) - (L_A/WVP_A)} \quad (2)$$

where *A*, *B* and *T* correspond to the A/C PET, to the five polysaccharide nanolayers and to the A/C PET with polysaccharide nanolayered coating, respectively. *L* corresponds to the thickness of the films. The thickness of A/C PET was measured by a digital micrometer (Mitutoyo, Japan) (100 μm) and the thickness of the polysaccharide nanolayered coating was determined by the SEM analyses.

### 3.6. Oxygen permeability

Oxygen permeability ($O_2P$) was determined based on the ASTM D3985-02 (ASTM D3985-02, 2002) method. The films were sealed between two chambers, having each one two channels. In the lower chamber $O_2$ was supplied at a constant flow rate controlled by a gas flowmeter (J & W Scientific, ADM 2000, USA) to maintain its pressure constant in that compartment. The other chamber was purged by a stream of nitrogen, also at controlled flow. Nitrogen acted as a carrier for the $O_2$. The flow leaving this chamber was connected to an $O_2$ sensor (Mettler Toledo, Switzerland) that measured $O_2$ concentration in that flow on-line.

The flows of the two chambers were connected to a manometer to ensure the equality of pressures (both at 1 atm) between both compartments. As the $O_2$ was carried continuously by the nitrogen flow, it was considered that partial pressure of $O_2$ in the upper compartment is null, therefore $\Delta P$ is equal to 1 atm. Three replicates were performed for each sample.

The polysaccharide nanolayers $O_2P$ were determined by the following equation (Cooksey, Marsh, & Doar, 1999):

$$O_2P_B = \frac{L_B}{(L_T/P_T) - (L_A/P_A)} \quad (3)$$

where A, B and T correspond to the A/C PET, to the five polysaccharide nanolayers and to the A/C PET with polysaccharide nanolayered coating, respectively. *L* corresponds to the thickness of the films. The thickness of A/C PET was measured by a digital micrometer (Mitutoyo, Japan) (100 μm) and the thickness of the nanolayered coating was determined by SEM.

### 3.7. Statistical analyses

The statistical analyses were carried out using analysis of variance, Tukey mean comparison test ($p < 0.05$) and linear regression analysis (SigmaStat, trial version, 2003, USA).

## 4. Results and discussion

### 4.1. Evaluation of the interactions between κ-carrageenan and chitosan

#### 4.1.1. Electrostatic properties of the polyelectrolytes

Since polyelectrolyte deposition is primarily governed by electrostatic interactions and in order to guarantee a correct interaction between the surface of the A/C PET and the κ-carrageenan nanolayer (the first one on the A/C PET surface) and between the subsequent κ-carrageenan/chitosan layers, it is necessary to assure that these polyelectrolytes exhibit opposite electrostatic properties. Therefore, to confirm the opposite charges of κ-carrageenan and chitosan solutions, their ζ-potential values were determined. The obtained values were $-56.90 \pm 5.11$ mV for κ-carrageenan solution at pH 7.0 and $+45.83 \pm 3.35$ mV for chitosan solution at pH 3.0, which means that these polyelectrolytes can interact by electrostatic forces. The ζ-potential values obtained for κ-carrageenan and chitosan solutions are in agreement with the ones obtained by Medeiros et al. (2011) ($60.53 \pm 0.15$ mV) and by Carneiro-da-Cunha et al. (2010) ($58.28 \pm 4.18$ mV), respectively.

Other pH values were tested for the κ-carrageenan and chitosan solutions (data not shown) and the pH values corresponding to the highest ζ-potential values were the ones chosen to perform the experiments in order to enhance the electrostatic interactions between these polyelectrolytes.

#### 4.1.2. Microcalorimetry analyses

Microcalorimetry is a thermodynamic technique that allows the study of the interactions between two species, by directly measuring the heat released or absorbed during a biomolecular binding event. Although the prevalent kind of interactions in our system is possibly electrostatic interactions, one of the objectives of this work is precisely to evaluate/confirm (through microcalorimetry) the specific energy of those interactions. Therefore, the measurement of the energy evolved or absorbed upon interaction between chitosan and κ-carrageenan compared to that obtained upon dilution of a concentrated chitosan solution can give thermodynamic information about the nature of the interactions between both polyelectrolytes (electrostatic, hydrogen bonds, van der Waals, among others). Whenever we refer to "interactions" in the subsequent text, we mean by default all types of interactions that may be occurring; the conclusion on the prevalent type of interaction in our system is presented at the end of this section. The curves of $\Delta H$ (resulting from the integration of the raw microcalorimetric data) (Denadai et al., 2006) *versus* total chitosan concentration added to water in the absence (dilution process, $\Delta_{dil}H$) and in the presence of a 0.2% (w/v) κ-carrageenan solution (dilution and interaction process, $\Delta_{obs}H$) are shown in Fig. 1a and b.

The titration curve for chitosan added to water (Fig. 1a) shows that in the concentration interval between 0 and 4.0 μmol $L^{-1}$ of chitosan, the dilution process of this polyelectrolyte is exothermic, with very low values of enthalpy of dilution in the range of $-0.59$ kJ $mol^{-1} < \Delta_{dil}H < -0.013$ kJ $mol^{-1}$. However, above 4.0 μmol $L^{-1}$, the dilution process becomes endothermic with the enthalpy of dilution having a value of 0.50 kJ $mol^{-1}$ for 6 μmol $L^{-1}$. The enthalpy changes obtained in these concentration intervals include mainly contributions from the decrease of chitosan–chitosan interaction (due to increase of distance between chitosan molecules during the dilution process—this increase of distance occurs when the concentrated chitosan solution is added to the water) and from the enthalpy changes due to modification of chitosan conformation/solvation. As the resulting enthalpy change is negative (exothermic) this means that the endothermic processes absorb less energy than the energy released by the exothermic processes. However, once $\Delta_{dil}H$ magnitudes are so small it is possible to conclude that both processes (endo and exothermic) have very similar absolute values of enthalpy change. The slope of the dilution curve is a measurement of the energy involved in the chitosan–chitosan interaction (i.e., the interaction between chitosan molecules). The system's enthalpy increases during the dilution process possibly due to changes in the repulsion of charges present on the double electric layers of the polyelectrolyte molecules.

The enthalpic curves for addition of chitosan solution into the κ-carrageenan aqueous solution are shown in Fig. 1b. The initial additions of chitosan solution result in exothermic enthalpy change values, caused by the intermolecular interaction between chitosan and κ-carrageenan macromolecules. The enthalpy change at 0.134 μmol $L^{-1}$ of chitosan is around $-19.8$ kJ $mol^{-1}$, showing an enthalpically favorable interaction. From Fig. 1b it can also be observed that all subsequent additions of chitosan to the

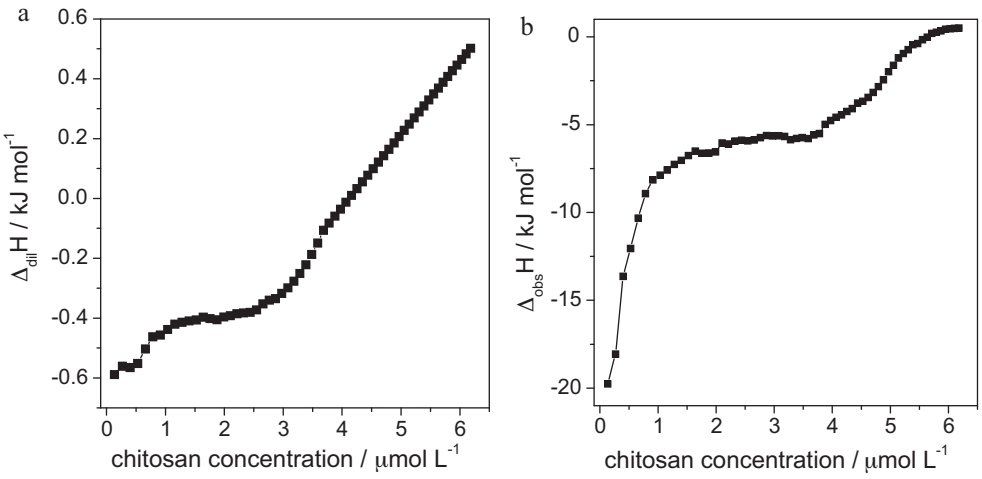


**Fig. 1.** (a) Dilution enthalpy change ($\Delta_{dil}H$) resulting from the titration of chitosan solution on water alone as function of chitosan solution concentration. (b) Observed enthalpy change ($\Delta_{obs}H$) resulting from the titration of chitosan solution on the κ-carrageenan solution as function of chitosan solution concentration.

κ-carrageenan solution lead to an exothermic effect, showing that in this concentration range chitosan macromolecules bind to κ-carrageenan and this interaction continues to be enthalpically favorable. However, when more chitosan is added, the interaction between the chitosan and κ-carrageenan becomes less exothermic. The slope of the $\Delta_{obs}H$ *versus* chitosan concentration plot is possibly caused by changes in the chitosan/κ-carrageenan interaction (reflected in changes in enthalpy), since for increasing chitosan concentrations, the free chitosan concentration decreases somewhat, and also by changes in aggregate–aggregate interactions with the increase of chitosan/κ-carrageenan aggregates' concentration. At a total chitosan concentration of 5.6 μmol L$^{-1}$, the κ-carrageenan chain became saturated with chitosan macromolecules, the influence of the κ-carrageenan on the dilution of chitosan solution in the calorimeter cell ceased, and $\Delta_{obs}H$ and $\Delta_{dil}H$ curves became equal. This critical concentration, defined as the concentration where the chitosan titration curve in κ-carrageenan solution joins the chitosan dilution curve in water corresponds to a concentration ratio ($r$) between chitosan and κ-carrageenan of 1.2 in the aggregates. The apparent enthalpy of interaction, $\Delta_{ap\text{-}int}H$, is equal to the enthalpy difference between $\Delta_{obs}H$ and $\Delta_{dil}H$ curves.

$$\Delta_{ap\text{-}int}H = \Delta_{obs}H - \Delta_{dil}H \quad (4)$$

For the application of [Eq. (4)], it must be kept in mind that the concentration of chitosan that is free in solution during the microcalorimetric titration experiment is different in the absence and in the presence of κ-carrageenan for the same total amount of chitosan added. As pointed out above, this difference occurs because a fraction of the added chitosan binds to κ-carrageenan. Therefore, the energy change caused by chitosan dilution will be just little different in the microcalorimetric experiments performed in the presence and absence of κ-carrageenan. As the amount of chitosan molecules bound per κ-carrageenan molecule is not known, it is not possible to calculate the exact molar enthalpy change of interaction, only an apparent molar enthalpy change, $\Delta_{ap\text{-}int}H$ (Barbosa et al., 2010). However, the features of the $\Delta_{ap\text{-}int}H$ curve are able to provide qualitative information about the progress of κ-carrageenan/chitosan interaction for increasing chitosan concentration. Due to the small contribution of chitosan dilution process enthalpy, the $\Delta_{ap\text{-}int}H$ curve between chitosan and κ-carrageenan is very similar to that obtained by addition of chitosan in the presence of κ-carrageenan. In Fig. 2 the $\Delta_{ap\text{-}int}H$ *versus* chitosan concentration values are shown for chitosan in the presence of 0.2% (w/v) κ-carrageenan aqueous solution.

The measured $\Delta_{ap\text{-}int}$H represents a superposition of the heat exchanges associated with different effects. In the initial additions of chitosan to the κ-carrageenan solution, chitosan dilution results in separation of chitosan macromolecules from each other, followed by chitosan interaction with κ-carrageenan. In the concentration interval studied, the $\Delta_{ap\text{-}int}H$ values are in the range of $-19.2\,\text{kJ mol}^{-1} < \Delta_{ap\text{-}int}H < 0.0\,\text{kJ mol}^{-1}$. The magnitude of this enthalpy change can be caused by electrostatic interactions as well as dipole–dipole, hydrogen bonds and conformation changes of both polyelectrolytes.

In order to evaluate the kind of κ-carrageenan/chitosan interactions on the A/C PET interface, titrations of chitosan solutions on a dispersion of κ-carrageenan adsorbed on the A/C PET powder particles were performed. The apparent enthalpy of interaction on A/C PET surface, $\Delta_{ap\text{-}int}H_{\text{A/C PET}}$, was obtained after the subtraction of the enthalpy change observed during titration of chitosan on κ-carrageenan/PET from that of the dilution of the chitosan solution. Fig. 3 shows the change in the apparent enthalpy of interaction between adsorbed κ-carrageenan/A/C PET and chitosan ($\Delta_{ap\text{-}int}H_{\text{A/C PET}}$) as a function of chitosan concentration.

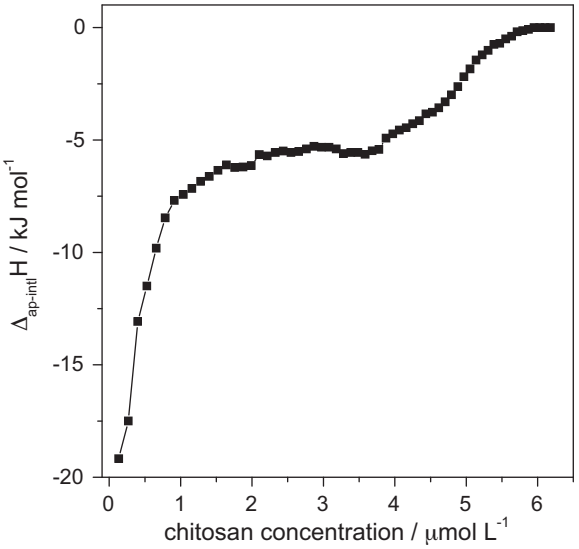


**Fig. 2.** κ-Carrageenan/chitosan apparent interaction enthalpy ($\Delta_{ap\text{-}int}H$) as a function of chitosan solution concentration.

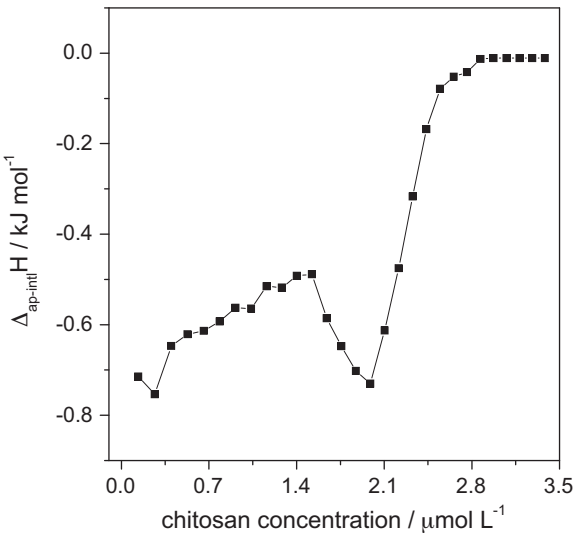


**Fig. 3.** Adsorbed A/C PET/κ-carrageenan/chitosan apparent interaction enthalpy change ($\Delta_{ap\text{-}int}H_{\text{A/C PET}}$) as a function of chitosan solution concentration.

For chitosan concentrations between 0.13 μmol L$^{-1}$ and 3.4 μmol L$^{-1}$, the values of $\Delta_{ap\text{-}int}H_{\text{A/C PET}}$ were in the range −0.71 kJ mol$^{-1}$ and −0.01 kJ mol$^{-1}$. Fig. 3 shows that, for lower chitosan concentrations (<1.5 μmol L$^{-1}$), $\Delta_{ap\text{-}int}H_{\text{A/C PET}}$ becomes slightly less negative, reaches a maximum value and then, in the vicinity of 1.5 μmol L$^{-1}$, abruptly decreases, remaining the adsorption process exothermic. This initial increase may arise from electrostatic interactions between chitosan and κ-carrageenan adsorbed as first layer on the A/C PET surface, while the abrupt decrease could be caused by changes in both polyelectrolytes conformation associated with film formation process (such as pH changes). After the minimum value of $\Delta_{ap\text{-}int}H_{\text{A/C PET}}$ (−0.73 kJ mol$^{-1}$) at 2.0 μmol L$^{-1}$ is attained, the addition of more chitosan promotes an abrupt increase in the adsorption energy of chitosan. This increase in the enthalpy of interaction could be attributed to the chitosan–chitosan interaction that occurs at surrounding sites on the κ-carrageenan/A/C PET surface, caused by the decrease in the distance between adsorbed chitosan molecules. These features suggest that the occurrence of the chitosan–chitosan interaction at that surface is the responsible by the formation of a dense film.

Moreover, when comparing the magnitude of $\Delta_{ap\text{-}int}H$ and $\Delta_{ap\text{-}int}H_{\text{A/C PET}}$ as a function of chitosan solution concentration (Figs. 2 and 3, respectively) it can be observed that the presence of the A/C PET causes a large decrease of the magnitude of the apparent enthalpy of interaction between κ-carrageenan and chitosan. This is possibly due to the electrostatic repulsion existing between A/C PET and chitosan molecules, once both exhibit positive charges. The influence of the substrate is eliminated only after more than 6–8 layers are deposited (Yoo, Shiratori, & Rubner, 1998).

### 4.1.3. Quartz crystal microbalance analysis

The real-time build-up of the κ-carrageenan and chitosan nanolayered assemblies is reported in Fig. 4a and b.

The decrease of the frequency after each polyelectrolyte deposition, observed in Fig. 4a, indicates that mass is being deposited at the crystal surface. $\Delta f$ changed from 0 to −20 Hz, from −67 to −156 Hz and from −186 to −293 Hz, after the adsorption of the first, second and third κ-carrageenan layer, respectively and changed from −19 to −70 Hz and from −156 to −192 Hz, after the deposition of the first and second chitosan layer, respectively. The adsorbed κ-carrageenan acts as a sublayer and offers binding sites for the subsequent chitosan adsorption and contrariwise,

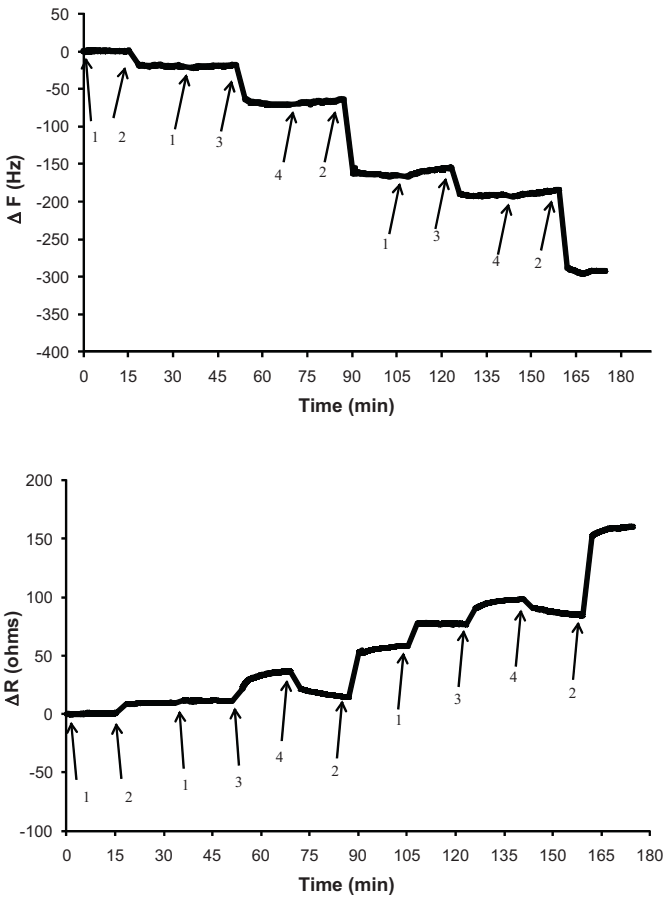


**Fig. 4.** Change in frequency (a) and in motional resistance (b) as a function of time for κ-carrageenan (0.2% (w/v), pH 7) and chitosan (0.2% (w/v), pH 3) adsorption and for rinsing with distilled water (pH 7 or pH 3); 1—distilled water at pH 7, 2—deposition of κ-carrageenan; 3—deposition of chitosan, 4—distilled water at pH 3.

therefore the $\Delta f$ caused by the adsorption of the first κ-carrageenan layer is significantly lower than the $\Delta f$ originated by the deposition of the following layers. Moreover, the roughness and the relative hydrophilicity of the substrate (crystal surface) affect the measurement of frequency and this effect is more pronounced in the first layer.

During the washing steps, the frequency did not decrease but remained stable, indicating that no desorption of the polyelectrolytes took place. From Fig. 4a it can also be concluded that the adsorption equilibrium is attained and stable films are obtained.

The decrease of frequency due to increasing film mass is accompanied by a resistance increase (Fig. 4b). The motional resistance represents the energy loss and the damping process within the system and is closely related to the physical properties of the adsorbed layers and adjacent liquid and its variation can be used to measure the viscoelastic change of the deposited film (Fakhrullin et al., 2007). From Fig. 4b it can be seen that the nanolayered κ-carrageenan/chitosan film dissipates energy, exhibiting viscoelastic behavior (Marx, 2003).

During deposition of mass on the QCM surface, an alteration in the hydrophilicity of the surface can result in higher frequency changes. From Fig. 4a and b it can be observed that the adsorption of κ-carrageenan results in higher changes in frequency and resistance compared with the adsorption of chitosan, which is possibly due to the more pronounced hydrophilic character of the κ-carrageenan. Hydrophilic surfaces (such as κ-carrageenan layer) are rough and can entrap solvents, resulting in a more viscoelastic multilayered system and contributing to the mass increase sensed

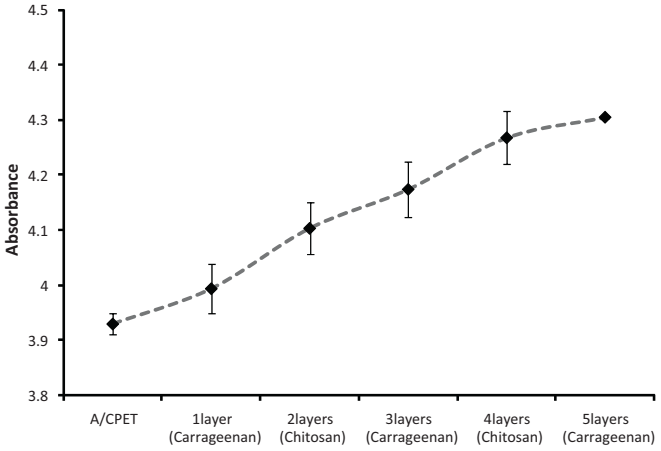


**Fig. 5.** Multilayer assembly monitored by UV/VIS spectroscopy at 260 nm. Each data point is the average of three determinations and the error bars show the standard deviation.

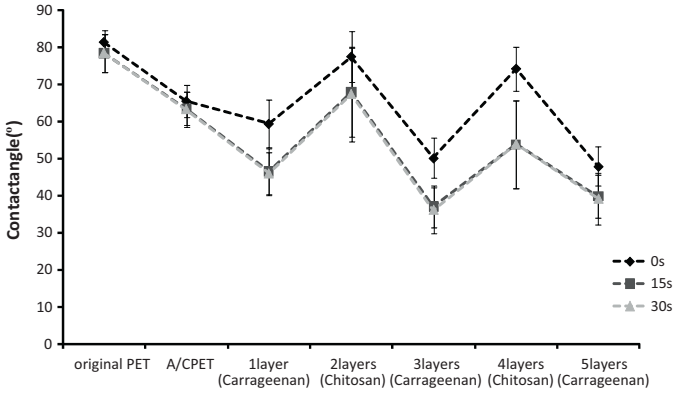


**Fig. 6.** Contact angle measurements for the original PET, the A/C PET and for the nanolayered coatings. The measurements were performed at 0, 15 and 30 s. Each data point is the average of ten measurements and the error bars show the standard deviation.

by the QCM and therefore to higher frequency changes. On the other hand, hydrophobic surfaces (such as chitosan layer) often do not wet and air can be entrapped, which results in smaller measured mass and energy losses. This is just one of the possibilities presented in the literature to explain the observed behavior; we advanced it as an hypothesis once a similar behavior has been previously observed by other authors (Martins, Mano, et al., 2010) for alginate/chitosan multilayered systems assembled by LbL technique.

It has to be taken into consideration that the mass corresponding to the frequency shift is the total adsorbed mass, which also includes the water entrapped in the adsorbed layer (Indest et al., 2008) and therefore a mass calculation can only be obtained for rigid thin films and was not performed in this work.

The QCM measurements confirm that the alternating deposition of κ-carrageenan and chitosan, at pH values in which polyelectrolytes carried opposite charge, results in the formation of a stable multilayer structure.

### 4.2. Characterization of the nanolayered coating

#### 4.2.1. UV/VIS spectroscopy

The multilayer coating growth on A/C PET surface was followed by UV/VIS spectroscopy. Fig. 5 shows the UV absorbance of κ-carrageenan/chitosan nanolayered coating plotted against the assembly step. The successful Layer-by-Layer deposition was confirmed by the increase in absorbance at 260 nm with an increasing assembly step. The multilayer growth has been characterized by a variety of growth regimes (e.g. linear and exponential) (Fu, Ji, Yuan, & Shen, 2005; Lavalle et al., 2002). Fig. 5 shows that, for the deposition of five layers, the amount of polyelectrolytes adsorbed on A/C PET surface is a linear function of the number of nanolayers.

#### 4.2.2. Contact angle measurements

The surface wettability of the nanolayered coating was investigated. The effect of the contact time between the drop and the surface of the coating was evaluated (Fig. 6) performing measurements at different contact times (after drop application). From Fig. 6 it can be concluded that the contact time does not influence the global trends. Also, the contact angles at 0 s for nanolayered coatings (from 1 to 5 layers) are notoriously different when compared to the values obtained at 15 and 30 s. On the other hand, the results obtained at 15 and 30 s are very similar, showing that there are no significant changes in the system for contact times above 15 s.

The hydrophobic character of the original PET substrate was confirmed by the high value obtained for its contact angle ($78.37 \pm 5.11^\circ$ at $t = 30$ s). This value is in good agreement with previous studies (Carneiro-da-Cunha et al., 2010; Xu, Wang, Fan, Ji, & Shen, 2008). After aminolysis, the PET surface exhibited a significantly ($p < 0.05$) lower contact angle ($63.21 \pm 4.81^\circ$ at $t = 30$ s), which means that the A/C PET is more hydrophilic than the original PET. Other authors (Xu, Wang, Fan, Ji, & Shen, 2008) reported a decrease in contact angle from $73.6 \pm 1.6^\circ$ to $61.8 \pm 1.0^\circ$ after the aminolysis of PET. Also, the difference obtained in contact angle between original and A/C PET confirms that the aminolysis process was correctly performed.

The contact angle results also show a distinct oscillation when the outermost layer changed between κ-carrageenan and chitosan, suggesting the progressive construction of the coating by alternate deposition of the nanolayers. The deposition of the κ-carrageenan layers induced a decrease in contact angle, whereas the deposition of chitosan led to the increase of contact angle. These results can be explained by the higher hydrophobicity of chitosan when compared to κ-carrageenan. This behavior is in agreement with the QCM measurements (Fig. 4). Since the outermost layer is κ-carrageenan, the produced coating exhibits a contact angle of approximately 40°, which makes it a relatively hydrophilic coating.

Moreover, the differences in wettability that were observed as the outermost layer changed between κ-carrageenan and chitosan may also be due to other factors besides the hydrophilicity of the functional groups of the adsorbed layer; such factors may include its chemical composition, the level of interpenetration of the outermost layer by segments of the previously adsorbed polymer layer (Yoo, Shiratori, & Rubner, 1998) and the swelling of the layers when in contact to water droplet. These are hypothesis than need to be confirmed by further work.

#### 4.2.3. Scanning electron microscopy (SEM)

Scanning electron microscopy (SEM) images of the different samples can be seen in Fig. 7. From these images it is possible to confirm the formation of the nanolayered coating on the A/C PET surface, corroborating the previous results. Comparing the surface of the original PET (Fig. 7a) and the surface of the nanolayered coating (Fig. 7b) allows significant differences to be seen. The surface of the nanolayered coating exhibits a more pronounced roughness and a higher number of particles, compared with the original PET surface.

Fig. 7c shows the first layer of κ-carrageenan and in Fig. 7d the two first layers (one of κ-carrageenan and one of chitosan) can be distinguished. SEM images allowed the estimation of the thicknesses of κ-carrageenan (37.9 nm) and chitosan (28.7 nm) layers and therefore of the 5 nanolayers (0.171 μm). However, since both

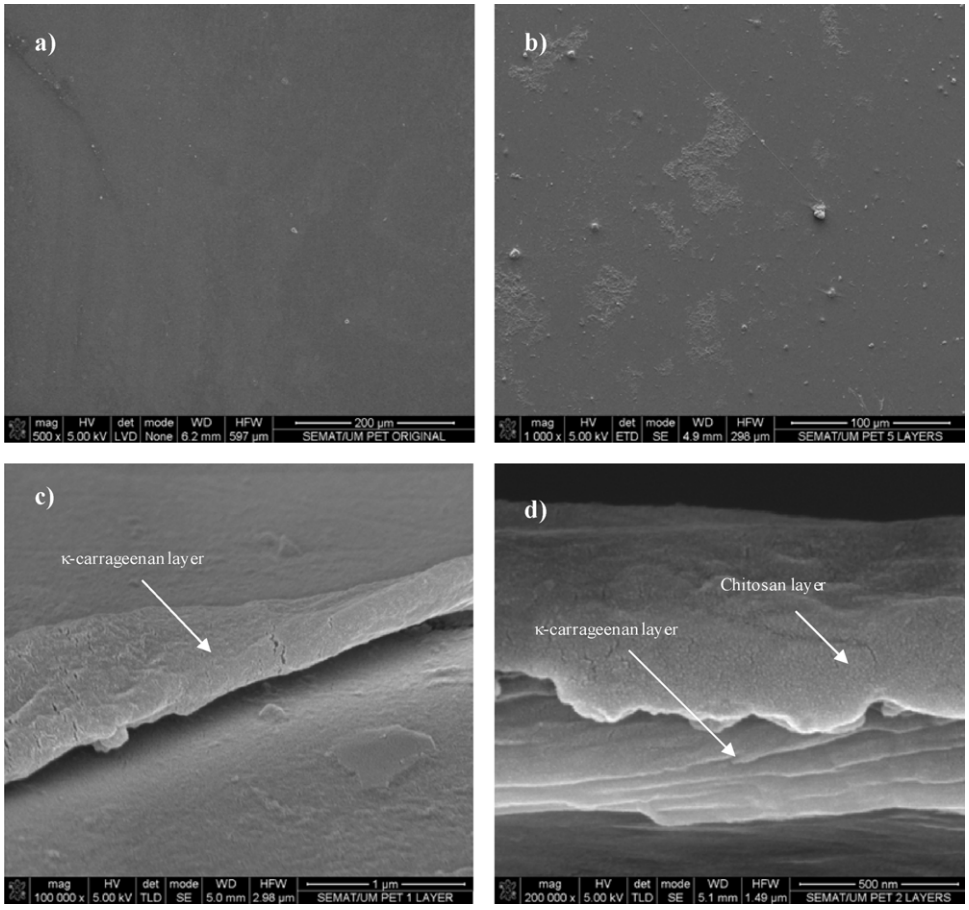


**Fig. 7.** SEM images of the surface morphology of the original PET (a); surface morphology of the A/C PET with the 5 nanolayers (b); first layer of κ-carrageenan (c); coating with two layers (κ-carrageenan and chitosan) (d).

sides of the A/C PET pieces were coated with the same set of layers, to obtain the total thickness it was necessary to multiply the obtained value by 2. Thus, the total thickness of the nanolayers is 0.342 μm.

### 4.2.4. Gas barrier properties

Gas barrier properties of the nanolayered coating were evaluated, using the A/C PET film as reference. The water vapor and oxygen permeabilities (WVP and $O_2P$, respectively) were measured and the results are shown in Table 1. The WVP values of the nanolayers were determined based on [Eq. (2)], using a thickness of 100 μm, which was measured by a micrometer, for the A/C PET and of 0.342 μm, measured by SEM, for the polysaccharide nanolayers.

Since the main function of food packaging is to avoid or decrease water loss, the WVP should be as low as possible (Gontard, Guilbert, & Cuq, 1992). Several factors have been shown to influence WVP, including film/coating composition, film/coating thickness and the technique used for film/coating preparation (Bifani et al., 2007). The produced nanolayers exhibited a lower WVP when compared with the values obtained for conventional edible films composed of chitosan ($WVP = (8.60 \pm 0.14) \times 10^{-11}$ g m$^{-1}$ s$^{-1}$ Pa$^{-1}$, ±50 μm of thickness) (Fajardo et al., 2010) and of sulfated polysaccharides such as ι-carrageenan (*WVP* between $(11.80 \pm 0.30) \times 10^{-11}$ and $(235 \pm 19.8) \times 10^{-11}$ g m$^{-1}$ s$^{-1}$ Pa$^{-1}$, depending on temperature and humidity gradient; ±50 μm of thickness) (Hambleton, Debeaufort, Beney, Karbowiak, & Voilley, 2008). Also, the κ-carrageenan/chitosan nanolayered coating exhibits a *WVP* very similar to the value obtained for an alginate/chitosan ($WVP = (0.014 \pm 0.001) \times 10^{-11}$ g m$^{-1}$ s$^{-1}$ Pa$^{-1}$, 0.12 μm of thickness) (Carneiro-da-Cunha et al., 2010) and κ-carrageenan/lysozyme ($WVP = (0.013 \pm 0.003) \times 10^{-11}$ g m$^{-1}$ s$^{-1}$ Pa$^{-1}$, 0.47 μm of thickness) (Medeiros, Pinheiro, Teixeira, Vicente, & Carneiro-da-Cunha, 2011) nanolayered coating, both also composed of five nanolayers.

The WVP is strongly governed by the interaction between polymer and water molecules. The hydrophobic character of chitosan nanolayers, confirmed by contact angle measurements, partially explains the lower WVP values of the nanolayers in comparison with the WVP value of A/C PET. These good results may also be explained based on interactions established between the κ-carrageenan and chitosan layers that lead to an increase of the tortuosity of the material and consequently to a decrease of the permeability to the water molecules (Jang, Rawson, & Grunlan, 2008; Tieke, Pyrasch, & Toutianoush, 2003). Finally, the fact that

**Table 1**
Water vapour permeability (*WVP*) and oxygen permeability ($O_2P$) of the A/C PET, of the PET with κ-carrageenan/chitosan nanolayers and of the nanolayers alone. The values represent the experimental average ± standard deviation.

| Sample | WVP × $10^{-11}$ (g m$^{-1}$ s$^{-1}$ Pa$^{-1}$) | $O_2P$ × $10^{-14}$ (g m$^{-1}$ s$^{-1}$ Pa$^{-1}$) |
|---|---|---|
| A/C PET | 2.07 ± 0.34 | 2.19 ± 0.81 |
| A/C PET + nanolayers | 1.53 ± 0.39 | 1.74 ± 0.35 |
| Nanolayers | 0.020 ± 0.002 | 0.043 ± 0.027 |

water molecules must cross several interfaces between the five nanolayers of material may also be contributing to the lower values of WVP.

The food quality can be improved and consequently, the food shelf life can be extended by the application of films/coatings with proper oxygen barrier properties, since the presence of oxygen may cause oxidation, which initiates several food alterations such as odor, color, flavor and nutrients deterioration (Sothornvit & Pitak, 2007).

The κ-carrageenan/chitosan nanolayered coating exhibits a $O_2P$ lower than a κ-carrageenan/lysozyme nanolayered coating ($O_2P = (0.1 \pm 0.01) \times 10^{-14}$ g m$^{-1}$ s$^{-1}$ Pa, 0.47 μm of thickness) (Medeiros, Pinheiro, Teixeira, Vicente, & Carneiro-da-Cunha, 2011) and than conventional edible films composed of chitosan ($O_2P = (0.71 \pm 0.02) \times 10^{-14}$ g m$^{-1}$ s$^{-1}$ Pa$^{-1}$, ±50 μm of thickness) (Fajardo et al., 2010) and of sulfated polysaccharides such as ι-carrageenan ($O_2P = (720 \pm 280) \times 10^{-14}$ g m$^{-1}$ s$^{-1}$ Pa$^{-1}$, ±50 μm of thickness) (Hambleton, Debeaufort, Beney, Karbowiak, & Voilley, 2008). Generally, polysaccharide films/coatings are good oxygen barriers, since their hydrogen-bonded network structure is firmly packed and arranged (Martins, Cerqueira, Souza, Avides, & Vicente, 2010).

## 5. Conclusions

The obtained results allowed concluding on the nature of interactions between κ-carrageenan and chitosan, two polyelectrolytes of opposite charges. Microcalorimetric measurements showed that the interaction between κ-carrageenan and chitosan is an exothermic process and that the formation of a nanolayered coating occurs mainly due to electrostatic interactions existing between the two polyelectrolytes, though other types of interactions such as dipole–dipole, hydrogen bonds and conformation changes of both polyelectrolytes may also be involved.

From the quartz crystal microbalance measurements it could be concluded that the alternating deposition of κ-carrageenan and chitosan results in the formation of a stable multilayer structure. The κ-carrageenan/chitosan nanolayers exhibit good gas barrier properties and therefore offer great potential to be used, e.g. to coat food systems. These results contribute to a deeper understanding of the interactions between the polyelectrolytes in a multilayer system and can be of utmost importance when considering the development of systems tailored for increasingly specific applications.

## Acknowledgements

The authors Ana C. Pinheiro and Ana I. Bourbon are recipient of fellowships from the Fundação para a Ciência e Tecnologia (FCT, Portugal) through grants SFRH/BD/48120/2008 and SFRH/BD/73178/2010, respectively. The Author Bartolomeu G. de S. Medeiros was recipient of a scholarship from de Project Isac (Isac Mundus Cooperation, European Union) and is also a recipient of a scholarship from Coordenação de Aperfeiçoamento de Pessoal de Nível Superior" (Capes, Brazil). The authors would like to acknowledge FINEP for the microcalorimeter and support by CAPES/PROCAD/1415/2007. The authors also acknowledge Dr. Edith Ariza from SEMAT/UM by the support in SEM analysis.

## References

ASTM D3985-02. (2002). Standard test method for oxygen gas transmission rate through plastic film and sheeting using a coulometric sensor. In *Annual book of ASTM*. Philadelphia, PA: Amer. Soc. for Testing & Materials.

ASTM E96-92. (1990). Standard test methods for water vapor transmission of materials. In *Annual book of ASTM standards*. Philadelphia, PA: Amer. Soc. for Testing & Materials.

Barbosa, A. M., Santos, I. J. B., Ferreira, G. M. D., da Silva, M. D. H., Teixeira, A. & da Silva, L. H. M. (2010). Microcalorimetric and SAXS determination of PEO-SDS interactions: The effect of cosolutes formed by ions. *Journal of Physical Chemistry B*, *114*(37), 11967–11974.

Begin, A. & Van Calsteren, M. R. (1999). Antimicrobial films produced from chitosan. *International Journal of Biological Macromolecules*, *26*(1), 63–67.

Bifani, V., Ramirez, C., Ihl, M., Rubilar, M., Garcia, A. & Zaritzky, N. (2007). Effects of murta (Ugni molinae Turcz) extract on gas and water vapor permeability of carboxymethylcellulose-based edible films. *LWT-Food Science and Technology*, *40*(8), 1473–1481.

Buttry, D. A. & Ward, M. D. (1992). Measurement of interfacial processes at electrode surfaces with the electrochemical quartz crystal microbalance. *Chemical Reviews*, *92*(6), 1355–1379.

Carneiro-da-Cunha, M. G., Cerqueira, M. A., Souza, B. W. S., Carvalho, S., Quintas, M. A. C., Teixeira, J. A., et al. (2010). Physical and thermal properties of a chitosan/alginate nanolayered PET film. *Carbohydrate Polymers*, *82*(1), 153–159.

Cooksey, K., Marsh, K. S. & Doar, L. H. (1999). Predicting permeability & transmission rate for multilayer materials. *Food Technology*, *53*(9), 60–63.

da Silva, L. H. M., da Silva, M. C. H., Francisco, K. R., Cardoso, M. V. C., Minim, L. A. & Coimbra, J. S. R. (2008). PEO–M(CN)$_5$NO$_x^-$ (M = Fe, Mn, or Cr) interaction as a driving force in the partitioning of the pentacyanonitrosylmetallate anion in ATPS: Strong effect of the central atom. *Journal of Physical Chemistry B*, *112*(37), 11669–11678.

Decher, G. & Schlenoff, J. B. (2003). *Polyelectrolyte multilayers, an overview*. Weinheim Wiley-VCH Verlag GmbH & Co. KGaA.

Denadai, A. M. L., Santoro, M. M., Da Silva, L. H., Viana, A. T., Santos, R. A. S. & Sinisterra, R. D. (2006). Self-assembly characterization of the beta-cyclodextrin and hydrochlorothiazide system: NMR, phase solubility, ITC and QELS. *Journal of Inclusion Phenomena and Macrocyclic Chemistry*, *55*(1-2), 41–49.

dos Santos, D. S., Riul, A., Malmegrim, R. R., Fonseca, F. J., Oliveira, O. N. & Mattoso, L. H. C. (2003). A layer-by-layer film of chitosan in a taste sensor application. *Macromolecular Bioscience*, *3*(10), 591–595.

Fajardo, P., Martins, J. T., Fucinos, C., Pastrana, L., Teixeira, J. A. & Vicente, A. A. (2010). Evaluation of a chitosan-based edible film as carrier of natamycin to improve the storability of Saloio cheese. *Journal of Food Engineering*, *101*(4), 349–356.

Fakhrullin, R. F., Vinter, V. G., Zamaleeva, A. I., Matveeva, M. V., Kourbanov, R. A., Temesgen, B. K., et al. (2007). Quartz crystal microbalance immunosensor for the detection of antibodies to double-stranded DNA. *Analytical and Bioanalytical Chemistry*, *388*(2), 367–375.

Fu, J., Ji, J., Yuan, W. & Shen, J. (2005). Construction of anti-adhesive and antibacterial multilayer films via layer-by-layer assembly of heparin and chitosan. *Biomaterials*, *26*(33), 6684–6692.

Gontard, N., Guilbert, S. & Cuq, J.-L. (1992). Edible wheat gluten films: Influence of the main process variables on film properties using response surface methodology. *Journal of Food Science*, *57*(1), 190–195.

Hambleton, A., Debeaufort, F., Beney, L., Karbowiak, T. & Voilley, A. (2008). Protection of active aroma, compound against moisture and oxygen by encapsulation in biopolymeric emulsion-based edible films. *Biomacromolecules*, *9*(3), 1058–1063.

Indest, T., Laine, J., Johansson, L. S., Stana-Kleinschek, K., Strnad, S., Dworczak, R., et al. (2009). Adsorption of fucoidan and chitosan sulfate on chitosan modified PET films monitored by QCM-D. *Biomacromolecules*, *10*(3), 630–637.

Indest, T., Laine, J., Ribitsch, V., Johansson, L.-S., Stana-Kleinschek, K. & Strnad, S. (2008). Adsorption of chitosan on PET films monitored by quartz crystal microbalance. *Biomacromolecules*, *9*(8), 2207–2214.

Jang, W. S., Rawson, I. & Grunlan, J. C. (2008). Layer-by-layer assembly of thin film oxygen barrier. *Thin Solid Films*, *516*(15), 4819–4825.

Lavalle, P., Gergely, C., Cuisinier, F. J. G., Decher, G., Schaaf, P., Voegel, J. C., et al. (2002). Comparison of the structure of polyelectrolyte multilayer films exhibiting a linear and an exponential growth regime: An in situ atomic force microscopy study. *Macromolecules*, *35*(11), 4458–4465.

Martins, J. T., Cerqueira, M. A., Souza, B. W. S., Avides, M. C. & Vicente, A. N. A. (2010). Shelf life extension of ricotta cheese using coatings of galactomannans from nonconventional sources incorporating nisin against listeria monocytogenes. *Journal of Agricultural and Food Chemistry*, *58*(3), 1884–1891.

Martins, G. V., Mano, J. F. & Alves, N. M. (2010). Nanostructured self-assembled films containing chitosan fabricated at neutral pH. *Carbohydrate Polymers*, *80*(2), 570–573.

Marx, K. A. (2003). Quartz crystal microbalance: A useful tool for studying thin polymer films and complex biomolecular systems at the solution-surface interface. *Biomacromolecules*, *4*(5), 1099–1120.

Medeiros, B., Pinheiro, A., Teixeira, J., Vicente, A. & Carneiro-da-Cunha, M. (2011). Polysaccharide/protein nanomultilayer coatings: Construction, characterization and evaluation of their effect on 'Rocha' Pear (*Pyrus communis* L.) shelf-life. *Food and Bioprocess Technology*, 1–11.

Park, S. Y., Lee, B. I., Jung, S. T. & Park, H. J. (2001). Biopolymer composite films based on [kappa]-carrageenan and chitosan. *Materials Research Bulletin*, *36*(3-4), 511–519.

Pranoto, Y., Rakshit, S. K. & Salokhe, V. M. (2005). Enhancing antimicrobial activity of chitosan films by incorporating garlic oil, potassium sorbate and nisin. *LWT-Food Science and Technology*, *38*(8), 859–865.

Rudra, J. S., Dave, K. & Haynie, D. T. (2006). Antimicrobial polypeptide multilayer nanocoatings. *Journal of Biomaterials Science-Polymer Edition*, *17*(11), 1301–1315.

Sauerbrey, G. (1959). Verwendung von Schwingquarzen zur Wägung dünner Schichten und zur Mikrowägung. *Zeitschrift für Physik A Hadrons and Nuclei*, *155*(2), 206–222.

Shi, P., Zuo, Y., Zou, Q., Shen, J., Zhang, L., Li, Y., et al. (2009). Improved properties of incorporated chitosan film with ethyl cellulose microspheres for controlled release. *International Journal of Pharmaceutics*, *375*(1-2), 67–74.

Sobral, P. J. A., Menegalli, F. C., Hubinger, M. D. & Roques, M. A. (2001). Mechanical, water vapor barrier and thermal properties of gelatin based edible films. *Food Hydrocolloids*, *15*(4-6), 423–432.

Sothornvit, R. & Pitak, N. (2007). Oxygen permeability and mechanical properties of banana films. *Food Research International*, *40*(3), 365–370.

Tieke, B., Pyrasch, M. & Toutianoush, A. (2003). Functional layer-by-layer assemblies with photo- and electrochemical response and selective transport of small molecules and ions. In G. Decher, & J. B. Schlenoff (Eds.), *Multilayer thin films: Sequential assembly of nanocomposite materials*. Weinheim Wiley–VCH Verlag GmbH & Co. KGaA.

Vinayahan, T., Williams, P. A. & Phillips, G. O. (2010). Electrostatic interaction and complex formation between gum Arabic and bovine serum albumin. *Biomacromolecules*, *11*(12), 3367–3374.

Wang, Y., Angelatos, A. S. & Caruso, F. (2007). Template synthesis of nanostructured materials via layer-by-layer assembly. *Chemistry of Materials*, *20*(3), 848–858.

Wasikiewicz, J. M., Yoshii, F., Nagasawa, N., Wach, R. A. & Mitomo, H. (2005). Degradation of chitosan and sodium alginate by gamma radiation, sonochemical and ultraviolet methods. *Radiation Physics and Chemistry*, *73*(5), 287–295.

Weiss, J., Takhistov, P. & McClements, D. J. (2006). Functional materials in food nanotechnology. *Journal of Food Science*, *71*(9), R107–R116.

Xu, J. P., Wang, X. L., Fan, D. Z., Ji, J. & Shen, J. C. (2008). Construction of phospholipid anti-biofouling multilayer on biomedical PET surfaces. *Applied Surface Science*, *255*(2), 538–540.

Yoo, D., Shiratori, S. S. & Rubner, M. F. (1998). Controlling bilayer composition and surface wettability of sequentially adsorbed multilayers of weak polyelectrolytes. *Macromolecules*, *31*(13), 4309–4318.

Ziani, K., Oses, J., Coma, V. & Maté, J. I. (2008). Effect of the presence of glycerol and Tween 20 on the chemical and physical properties of films based on chitosan with different degree of deacetylation. *LWT-Food Science and Technology*, *41*(10), 2159–2165.